

# Effect of absorption on light scattering by agglomerated debris particles

Evgenij Zubko,<sup>1,2</sup> Hiroshi Kimura,<sup>3</sup> Yuriy Shkuratov,<sup>2</sup> Karri Muinonen,<sup>4</sup>  
Tetsuo Yamamoto,<sup>3</sup> Hajime Okamoto,<sup>1</sup> and Gordon Videen<sup>5</sup>

<sup>1</sup> *Graduate School of Science, Tohoku University, Japan;* <sup>2</sup> *Institute of Astronomy, Kharkov National University, Ukraine;* <sup>3</sup> *Institute of Low Temperature Science, Hokkaido University, Japan;*  
<sup>4</sup> *Observatory, University of Helsinki, Finland;* <sup>5</sup> *Space Science Institute, USA*

**Abstract.** We study the influence of material absorption on light scattering by agglomerated debris particles whose sizes are comparable with the wavelength. We find that the angular profile of linear polarization is extremely sensitive to the imaginary part of refractive index, and there are some unique features that may assist in the retrieval of physical properties of particles using remote-sensing techniques. Most notably, the position of the positive polarization maximum  $\alpha_{\max}$  changes monotonically with the imaginary part of refractive index, allowing it to be used to characterize this property. In addition, the amplitude of the negative polarization branch (NPB) is significantly greater for dielectric particles than for non-dielectric particles. It disappears in the transition region between dielectric and conducting particles before reappearing as the imaginary part of the refractive index is increased further. Further increasing the imaginary part of the refractive index may see the NPB disappearing and reappearing in quasi-periodic fashion. This recurrent NPB has a much smaller amplitude than that of dielectric particles. This suggests that the cometary circumnuclear haloes, which have significant NPBs, cannot contain significant quantities of absorbing particles. In addition, combined observations suggest that the polarization maximum of circumnuclear haloes are relatively small  $P_{\max} \sim 12\%$ , and occur at relatively small phase angles  $\alpha_{\max} \sim 60^\circ$ , which is also consistent with dielectric particles.

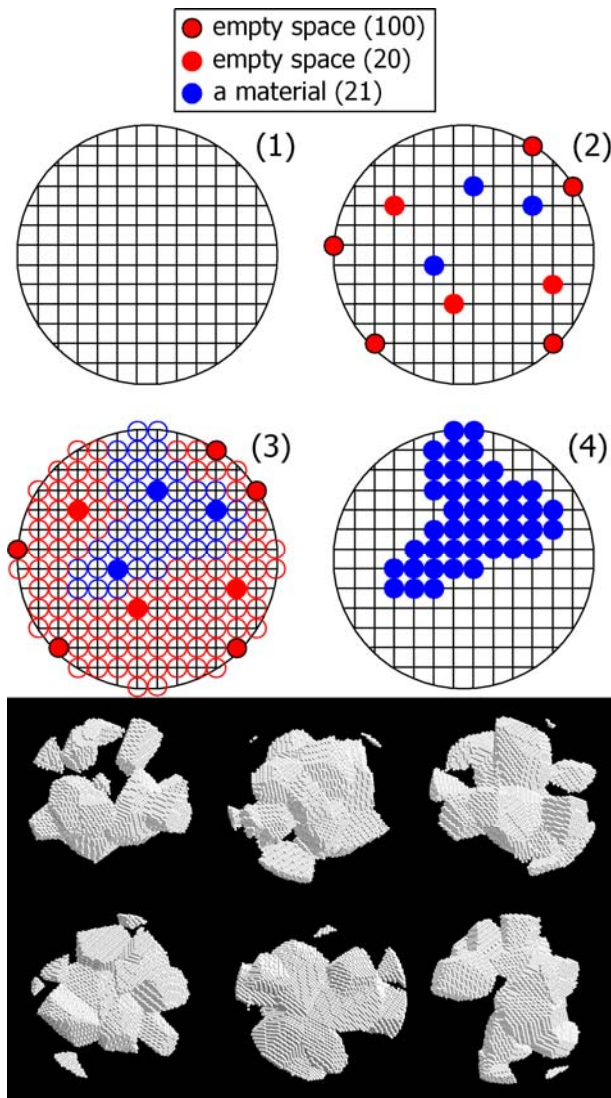


Figure 1

## Model of agglomerated debris particles

We simulate the light scattered by irregularly shaped particles using our implementation of the discrete dipole approximation (DDA) (see, e.g., [1–4]). We generate irregularly shaped model particles by damaging a perfect sphere with the following algorithm (see Fig. 1). A spherical volume is filled with a regular cubic lattice that is considered as the initial matrix of the irregular particles. All cubic cells forming this initial matrix are divided into two groups: cells belonging to the surface layer and cells internal to the surface layer. Among surface dipoles, we choose randomly 100 cells that are considered as seed cells of empty space. In the set of internal dipoles, we randomly choose 21 seed cells of material and 20 seed cells of empty space. Then, step-by-step, each cell distinct from the seed cells is marked with the same optical properties as that of the nearest seed cell. Images of six sample particles generated in this way are shown in the bottom of Fig 1. As can be seen, the particles appear to be agglomerates of very irregular shape. We identify such particles as agglomerated debris particles.

The total numbers of cells forming the initial matrices are 17,256, 137,376 and 1,099,136; the choice depends on size parameter  $x$ . Material in these agglomerated debris particles occupies on average approximately 26% of these volumes; thus, these agglomerated debris particles have a rather sparse structure.

Previously, we have studied the light scattering of some manifestations of this kind of particles [2–4].

## Results and Discussion

We consider a set of four size parameters  $x = 5, 10, 20,$  and  $30$  ( $x = 2\pi r_{cs}/\lambda$ , where  $r_{cs}$  is radius of circumscribing sphere,  $\lambda$  – wavelength). In the simulations, the real part of the refractive index has been fixed at 1.5. Excluding the case of  $x = 30$ , the imaginary part is varied from 0 to 1.3. For the largest particles convergence cannot be reached at

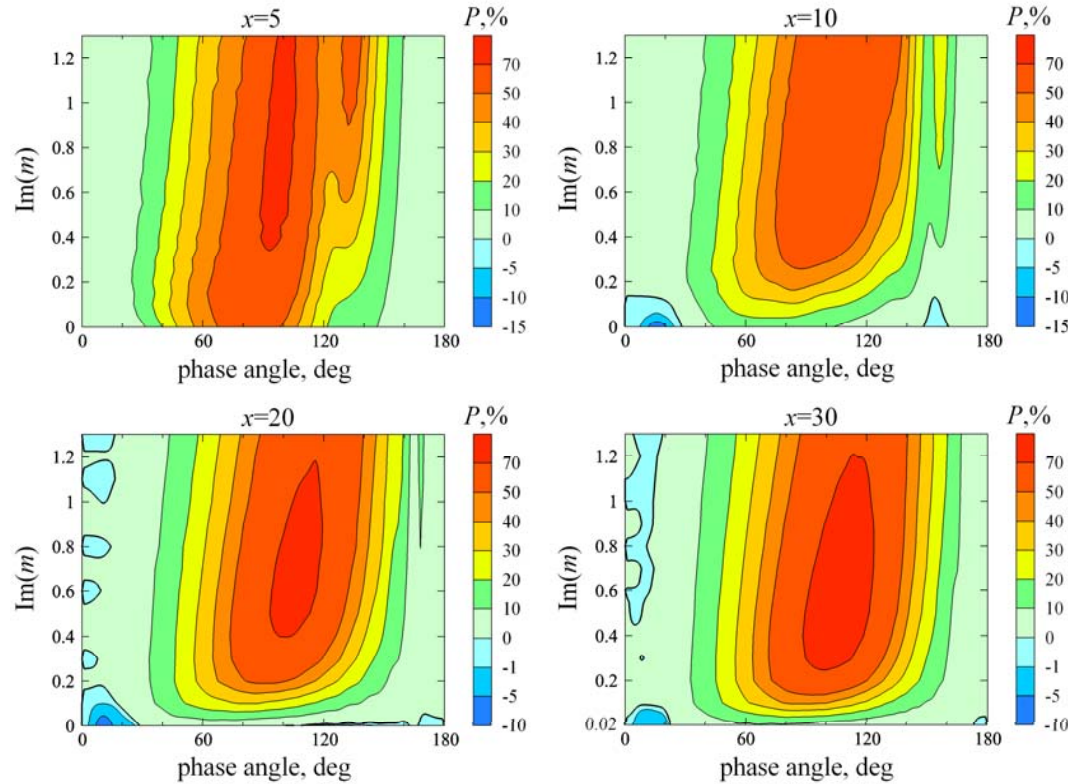


Figure 2

$\text{Im}(m) = 0$ . For averaging, we consider a minimum of 500 particle realizations for each size parameter. Scattering properties of each particle have been averaged additionally over 100 scattering planes, evenly distributed around the wavevector of the incoming light.

Fig. 2 shows the degree of linear polarization  $P$  (corresponding to the ratio of Mueller matrix elements  $-S_{21}/S_{11}$ ) as a function of phase angle  $\alpha$  and the imaginary part of refractive index  $\text{Im}(m)$ . Four panels are shown for size parameters ranging from  $x = 5$  to  $x = 30$ . One can see that the smallest particles show only positive linear polarization at all phase angles. When  $\text{Im}(m)$  exceeds 0.5, the angular profiles of linear polarization of the small particles are bimodal and further increasing  $\text{Im}(m)$  makes this effect more explicit. This feature is most

pronounced in the case of the smallest particles ( $x = 5$ ) studied as increasing particle size tends to wash it away as does decreasing particle size. At  $x = 30$ , the second maximum is already inexpressive. It is interesting to note that a similar bimodal profile of the polarization curve can be seen in laboratory measurements of hematite particles [5].

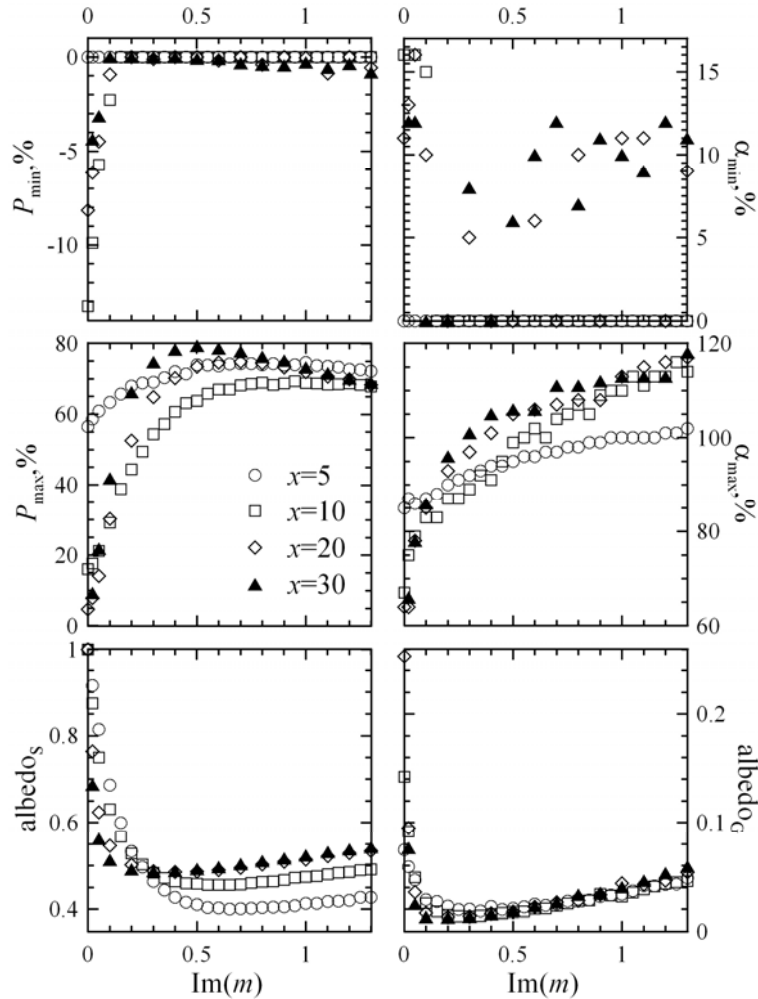


Figure 3

3, single-scattering albedo is visibly better correlated with the inverse of  $P_{\max}$  rather than geometrical albedo. Nevertheless, for both types of albedo, there is a range of  $\text{Im}(m)$  where the inverse correlation with the maximum of positive polarization fails. For both albedos, this occurs for transient materials, but in the case of single-scattering albedo, the range at which the inverse correlation fails is smaller in  $\text{Im}(m)$ .

In general, the polarization maximum  $P_{\max}$  depends non-monotonically on  $\text{Im}(m)$  (see also Fig. 3). The largest polarizations tend to occur in the transition zone between dielectric and conducting particles. Increasing the particle size tends to make it more pronounced. Unlike  $P_{\max}$ , the phase angle of maximum polarization  $\alpha_{\max}$  increases monotonically with  $\text{Im}(m)$ . The range of variation increases with particle size. Potentially, this may be an indicator of particle absorption.

Both single-scattering and geometrical albedos (see bottom panels in Fig. 3) reveal an inverse correlation with the positive polarization maximum  $P_{\max}$ . The later parameter is defined as the ratio of the energy scattered at phase angle  $0^\circ$  to that scattered by a white Lambert disk of the same geometric cross-section ( $\text{albedo}_G = (S_{11}\pi)/(k^2G)$ , where  $S_{11}$  is the element of Mueller matrix,  $k$  – wavenumber and  $G$  – geometrical cross-section of the particle). Note that, the term “geometrical albedo” is more appropriate to describe light-scattering properties of surfaces; whereas, in the case of independent particles, it is just intensity at backscattering which is normalized. Nevertheless, the geometrical albedo is being actively used in the cometary physics, and, therefore, we consider this parameter here. As one can see in Fig.

Our simulations demonstrate a negative polarization branch (NPB) at small phase angles that depends strongly on size parameter and material absorption. This feature is a region of negative polarization at very small yet non-zero phase angles, extending out to  $10^\circ$ - $20^\circ$ . It is not visible for the smallest particles ( $x = 5$ ), but appears for larger particles and becomes more persistent as size parameter increases. Interestingly, at  $\text{Re}(m) = 1.5$  there is a strong NPB for very low absorption that completely disappears for all considered particles as  $\text{Im}(m) > 0.1$ . When the size parameter of the particles is larger than  $x = 20$ , the negative polarization reappears again at larger values of  $\text{Im}(m)$ . However, in all cases, this feature is no longer as deep as for particles having very low absorption. The position of the NPB minimum does not reveal a systematic behavior when the particles are in the dielectric domain, but in the transient and conductive domains, i.e.  $\text{Im}(m) > 0.1$ , it tends to shift to larger phase angles. This resurgent NPB may

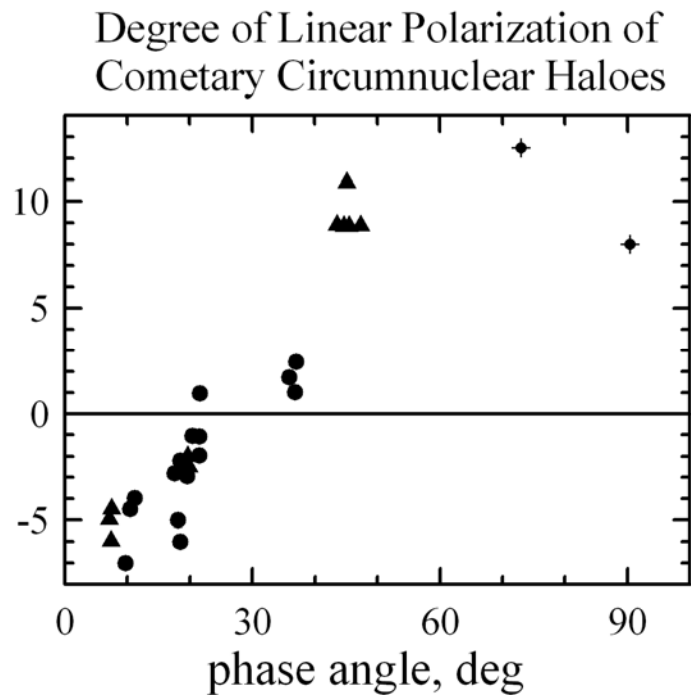


Figure 4

also disappear and reappear quasi-periodically with increasing absorption (e.g.,  $x = 20$ ). The depth of the NPB remains approximately the same for these larger absorptions and is much smaller than for the very low absorption case, suggesting that it may have a different physical mechanism than that of the near-dielectric particles. Notice also that the NPB for the more absorbing particles often are periodically accompanied by a positive polarization branch (PPB) near  $\alpha = 0$  (e.g.,  $x = 20, 30$ ). Considering the specific properties of conductors, we can guess that, in this case, the negative polarization may appear due to surface waves.

The dependence of the NPB on  $\text{Im}(m)$  leads us to one very important conclusion concerning the properties of dust in cometary circumnuclear haloes. Those haloes are relatively small but bright clouds surrounding cometary nuclei. Polarimetry of comets demonstrates that the haloes have a very deep NPB at small phase angles [6–8] (see Fig. 4). Different comets show similar behavior: the minimum polarization  $P_{\min}$  is typically -6%.

Using results of our simulations, we can immediately derive threshold value for  $\text{Im}(m)$  that is approximately 0.05: if the imaginary part of the refractive index is greater than this value, then it is impossible to achieve such a deep negative polarization. Additionally, we must consider that our results concern only particles monodispersed in size; whereas, cometary particles are in all likelihood polydispersed in size, which would further reduce the depth of the minimum, especially since very small particles do not display any NPB. This suggests that the threshold of  $\text{Im}(m)$  is on the order of 0.02, corresponding to the relatively deep initial NPB. The results of the imaging polarimetry of comets coupled with our phase curves allow us to place restrictions on the materials present in the circumnuclear haloes.

*In situ* measurement of dust of comet 1P/Halley has shown that two the most abundant components are so-called ROCK and CHON [9]. ROCK corresponds to magnesia-rich silicates; whereas, CHON is a mixture of four chemical elements: carbon, hydrogen, oxygen, and nitrogen. The origin of CHON remains unclear, and there is an objective reason for this, since these four basic elements form a huge number of combinations. Even primitive meteorites reveal over 650 individual organic molecules [10]; therefore, the determination of optical constants of organic material could be quite helpful, at least, in order to reduce the number of variables concerning the organic material. From the restriction on the imaginary part of refractive index discussed above, we can conclude that the organic material based on that of the Greenberg model [11] cannot exist in considerable quantities in the circumnuclear haloes; neither can hydrogenated carbon [12]. The reason is that their absorption properties are too great and their significant presence would dampen the NPBs beyond what has been measured and recorded in the polarimetric images. We cannot rule out the presence of ice tholin [13] and kerogen [14] in significant quantities, since these have significantly lower absorption. We would like to stress that we do not claim that the organic material proposed by the Greenberg model and/or hydrogenated carbon are totally absent in comets, but only that it does not make up a significant proportion of their circumnuclear haloes. Indeed, the circumnuclear haloes are not the only features in polarimetric images of comets; there are also jets, which remain positively polarized over the entire range of phase angles [6].

The conclusion that dust particles in circumnuclear haloes are primarily weakly absorbing allows us to estimate the location and amplitude of the maximum of the positive polarization  $P_{\max}$ . At large phase angles, ground-based observations of circumnuclear haloes are met with a fundamental difficulty, since large phase angles can only be achieved when the distance from the comet to the Sun is comparatively small. When the comet is close to the sun it becomes very active and its circumnuclear halo is partially or completely hidden by jets [6]. Because of this difficulty, there are only two polarimetric measurements of circumnuclear haloes at large phase angles; both have been made with the Optical Probe Experiment (OPE) on board of Giotto space probe. The first measurement corresponds to comet 1P/Halley at a phase angle of 73 degrees [7]; whereas, the second corresponds to comet 26P/Grigg-Skjellerup at a phase angle of 90.4 degrees [8]. In Figure 4 we compile these data with those obtained using ground-based polarimetry of circumnuclear haloes [6]. The data suggests the location of the maximum of positive polarization from circumnuclear haloes to be located in the vicinity of  $\alpha_{\max} = 60^\circ$ , with  $P_{\max}$  being approximately 12%. Note that both the position and amplitude of the positive polarization for the circumnuclear haloes are consistent with the dielectric particles shown in Figure 3. When aperture-averaged polarimetry of the entire cometary comae is performed [6], the estimation of  $\alpha_{\max}$  approaches 100–110°, which is well beyond what can be expected from the data of Figure 4, suggesting that the particles in the circumnuclear halo are significantly different from the particles in the rest of the comae.

## References:

1. Zubko et al. 2003, *Opt Lett*, **28**, 1504.
2. Zubko et al. 2005, *Appl Opt*, **44**, 6479.
3. Zubko et al. 2006, *JQSRT*, **101**, 416.
4. Zubko et al. 2008, *JQSRT*, **109**, 2195.
5. Muñoz et al. 2006, *A&A*, **446**, 525.
6. Hadamcik & Levasseur-Regourd 2003, *JQSRT*, **79-80**, 661.
7. Levasseur-Regourd et al. 1999, *A&A*, **348**, 636.
8. Renard et al. 1996, *A&A*, **316**, 263.
9. Jessberger 1999, *Space Sc. Rev.*, **90**, 91.
10. Llorca 2005, *Int. Microbiol.*, **8**, 5.
11. Jenniskens 1993, *A&A*, **274**, 653.
12. Duley 1984, *ApJ*, **287**, 694.
13. Khare et al. 1993, *Icarus*, **103**, 290.
14. Khare et al. 1990, *LPSC-XXI*, 627.